JOURNAL
OF THE AMERICAN CHEMICAL SOCIETY

VOLUME 101, NUMBER 5 FEBRUARY 28, 1979

The Transition from Phase Waves to Trigger Waves in a Model of the Zhabotinskii Reaction

Edward J. Reusser[1] and Richard J. Field*

Contribution from the Department of Chemistry, University of Montana, Missoula, Montana 59812. *Received December 17, 1977*

Abstract: In principle, two kinds of traveling waves of chemical activity may occur during the ferroin-catalyzed oxidation of malonic acid by bromate ion. The first of these, called a phase wave, propagates independently of diffusion along a phase gradient in an oscillatory reagent. The second of these, called a trigger wave, propagates by means of the interaction of chemical reaction and diffusion of intermediate species in an excitable reagent. An oscillatory reagent is also excitable. A model of the chemistry occurring in this reaction has been proposed. It is shown here that the partial differential equations describing the dynamics of the interaction of reaction and diffusion in this model possess solutions corresponding to both phase waves and trigger waves. These equations are solved numerically using a finite difference implementation of the method of lines. Our results show that phase waves appear only in an oscillatory reagent and travel at a velocity equal to the reciprocal of the phase gradient which they are propagating along. The range of possible phase wave velocities in a particular reagent is very large. Trigger waves appear in either an oscillatory or merely excitable reagent. In a nonoscillatory, but excitable, reagent they travel at a unique velocity defined by the reactive and diffusive properties of the system. In an oscillatory reagent, trigger wave velocity may be variable as a result of spatial gradients in bromide ion concentration residual from an initially present phase gradient. If a phase wave is moving more slowly than a trigger wave would move under the same conditions, then the phase wave will initiate this trigger wave. Calculated trigger wave velocities agree satisfactorily with the observed value.

Introduction

The metal ion catalyzed oxidation and bromination of certain organic compounds by bromate ion is referred to as the Belousov-Zhabotinskii (BZ) reaction.[2] The organic materials used normally contain at least one enolizable hydrogen, and the reaction is run in an aqueous medium of pH ~0. The basic mechanistic features of the reaction were originally elucidated by Field, Körös, and Noyes[3] (FKN). Field[4] has recently reviewed the present level of detailed understanding of this mechanism. Edelson, Noyes, and Field[5] have carried out an updated computer simulation of a detailed FKN mechanism. It will be assumed here that readers have at least a rudimentary understanding of this mechanism.

The BZ reaction exhibits perhaps the broadest range of complex dynamic behavior of any known nonbiochemical reaction. While the overall reaction monotonically converts reactants (bromate ion and the organic material) into a broad spectrum of products, the ratio of the concentrations of the oxidized and reduced forms of the metal ion catalyst (present in an amount much less than the principal reactants) and the concentrations of various intermediates, including bromide ion and bromous acid ($HBrO_2$), may exhibit nonmonotonic (oscillatory) behavior. The types of nonmonotonic behaviors possible have been reviewed by Field.[4] Here we are concerned with perhaps the most striking of these phenomena: the appearance of highly structured traveling waves of chemical activity in a thin (2 mm) layer of unstirred reagent. Within these moving bands the ratio of the concentrations of the oxidized and reduced forms of the catalyst and the concentrations of some intermediates are grossly different than those in other parts of the reagent. These waves were first described by Zaikin and Zhabotinskii[6] and are most striking when ferroin[7] is used as the catalyst. They have also been observed in reagents in which cerium[8] or manganese[9] ion is used as the catalyst. The ferroin catalyzed system will be referred to as Z reagent and is the object of this investigation. The waves appearing in this system have been characterized by Field and Noyes[10] and especially by Winfree.[11] Normally waves appear at a point in the reagent referred to as a "pacemaker center" and propagate outward from that point in the form of a circle. Successive appearance of waves at a single pacemaker center produces a set of concentric rings or a "target pattern" such as is illustrated in Figure 1. Winfree has published striking photographs[11g] of these waves and has investigated the spiral or scroll-shaped structures[11a-d,f,g] that develop when a traveling wave is broken by physical shearing of the supporting Z reagent.

Phase and Trigger Waves. Traveling waves in various media are well known to physicists, mathematicians, biologists, and now to chemists. However, the mechanism of wave propagation normally familiar to physicists and mathematicians is quite different from that normally familiar to biologists and chemists. This has led to some confusion concerning the origin of the Z reagent waves. The two types of waves are referred to as phase waves and trigger waves. Winfree[11c] insisted that the difference between the two types of waves be recognized, and he[11e] eventually demonstrated experimentally that waves with characteristics of both types may appear in a Z reagent.

0002-7863/79/1501-1063$01.00/0

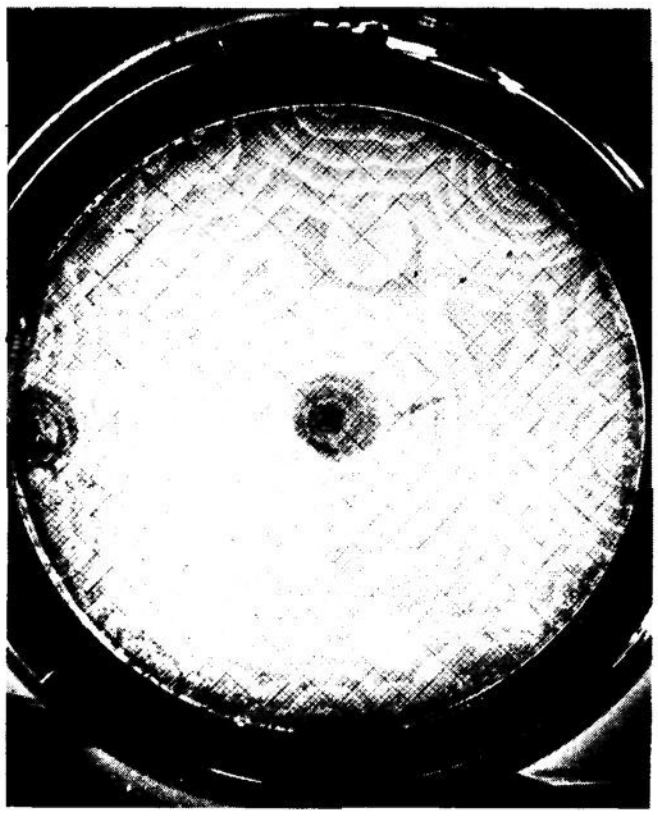

Figure 1. A typical set of concentric traveling waves in a thin layer of Z reagent. A Nichrome wire at the center is serving as the pacemaker. $[H_2SO_4]_0 = 0.26$ M, $[NaBrO_3]_0 = 0.23$ M, [malonic acid]$_0 = 0.024$ M, [bromomalonic acid]$_0 = 0.075$ M, [ferroin]$_0 = 5.45 \times 10^{-3}$ M, temperature = 25 °C. (Reproduced by permission from ref 10.)

Phase waves and trigger waves often can be distinguished from each other because the former are diffusion independent but dependent upon an at least potentially oscillatory medium for their propagation while the latter depend upon diffusion and upon an excitable, but not necessarily oscillatory, medium for propagation. For some reagent concentrations, the Z reagent can be both oscillatory and excitable while for others it is merely excitable.

Phase Waves. When a Z reagent is oscillatory its chemical kinetic steady state is unstable with respect to another kinetic state in which the ratio of the concentrations of the oxidized and reduced forms of the catalyst and the concentrations of several intermediate species oscillate in time. This state rather than the steady state is observed experimentally. If a sample of Z reagent is well stirred, concentrations of all chemical species are the same in all parts of the reagent. The oscillations are controlled by mass action kinetics; so such a well-stirred Z reagent will oscillate synchronously throughout its volume. The oscillations proceed with unique and reproducible frequency and amplitude for each set of reactant concentrations. The oscillation period may range from a few tenths of a second[12] to several minutes.[3] Because ferroin[7] is used as the catalyst in the Z reagent, reagent color oscillates between red (ferroin) and blue (ferriin) as the oxidized and reduced forms of the catalyst alternately predominate. These are relaxation oscillations and are thus far from sinusoidal. Essentially all oxidation of ferroin to ferriin occurs during a pulse that lasts for less than 1% of the oscillatory cycle. Thus the transition from red to blue occurs suddenly. Ferriin is then reduced back to ferroin over a further 10–20% of the cycle. The reagent then remains red until the next burst of ferroin oxidation.

In an unstirred reagent, however, there is no requirement for all parts of the reagent to oscillate synchronously. This fact is the basis of the appearance of phase waves. Imagine a line of isolated, adjacent points in a ferroin-catalyzed oscillatory reagent. Further imagine that the first point in the line is exactly at the phase of its cycle where the sudden change from red to blue occurs and that the phase of each successive point on the line is displaced to longer and longer times before the sudden shift from red to blue occurs. Then, as time passes, points will turn from red to blue successively down the line at a rate determined by the phase gradient along the line of points. An observer of the system will simply see a blue wave apparently traveling through the reagent. This is a pure phase wave. Nothing actually moves as a phase wave propagates. Thus there is no maximum velocity at which a phase wave can travel. We shall see, however, that in the Z reagent there is a minimum velocity. It is apparent that phase waves must pass through a point in space at the frequency of temporal oscillation at that point. Furthermore, because phase wave propagation does not rely upon the physical interchange of material between adjacent points, phase waves can appear to pass through a barrier impenetrable to diffusion. The traveling waves which appear when the Belousov–Zhabotinskii reaction itself is run in a cylinder rather than in a thin layer have been shown by Kopell and Howard[13] to pass through an impenetrable Plexiglass barrier. They thus behave as phase waves. Thoenes[14] has also shown experimentally that these waves behave as phase waves. Both authors treated the phase waves mathematically, and in both sets of experiments the required phase gradients were introduced as part of the experimental procedure.

Winfree,[11a] however, pointed out that the concentric rings which appear in the thin-layer experiments with the Z reagent cannot all be phase waves. Kopell and Howard[13] also recognized this fact. There are two principal reasons why this must be true. The first of these is that the rings appear spontaneously without any effort to establish a circular phase gradient. The second of these is that a thin layer of Z reagent in contact with the air is in fact not oscillatory. Under that circumstance, the target patterns persist and are more striking than in an oscillatory reagent. These then cannot be phase waves and must therefore be another sort of wave.

Trigger Waves. When a Z reagent is not oscillatory, its steady state is stable. Thus we not only expect the concentrations of reactants and products to be uniform throughout the reagent, but we also expect the concentrations of intermediates to be uniform and at their steady-state values in all unperturbed areas of the reagent. These steady-state concentrations will depend upon the concentrations of the major constituents of the reagent. Traveling waves may still appear in such a reagent. These are referred to as trigger waves. While trigger waves do not require an oscillatory medium, their propagation is diffusion dependent. Thus they cannot pass through impenetrable barriers. In order for trigger waves to appear, two requirements must be met. The first is that the reagent be excitable in the sense that small but finite changes in the concentrations of certain species can trigger enormously amplified changes in the concentrations of these species. The second requirement is intimately related to the first. It is the presence of very steep spatial concentration gradients in those species able to trigger amplification. In the Z reagent these gradients develop when a pulse of oxidation of ferroin to ferriin occurs at a point in the reagent. In the case of a nonoscillatory Z reagent with a stable but excitable kinetic steady state, the initial pulse occurs at a pacemaker center probably as the result of heterogeneous catalysis at a physical imperfection such as a gas bubble, dust mote, etc. It is possible to arrange artificial pacemakers such that trigger waves can be initiated or suppressed at will.[15] Within an area experiencing such a pulse, the concentration of $HBrO_2$ is about 10^5 times higher and that of Br^- 10^5 times lower than in adjacent areas not experiencing the pulse. This produces steep concentration gradients in these species. Furthermore, it is a decrease in Br^- concentration or increase in $HBrO_2$ concentration that triggers a pulse of ferroin oxidation in the excitable reagent. Thus diffusion of Br^- and $HBrO_2$ across their concentration gradients can trigger the pulse of ferroin oxidation in adjacent areas. By this mechanism a trigger wave of ferroin oxidation propagates through the medium. The velocity of trigger wave propagation is apparently

controlled by the rates of chemical reaction and diffusion. Thus trigger waves are expected to travel at a characteristic velocity in a nonoscillatory Z reagent of particular composition. After passage of a trigger wave, such a Z reagent decays back to its stable but excitable steady state. Concentric waves can occur in a nonoscillatory Z reagent only by multiple initiation of waves at the pacemaker center. Trigger waves pass through a point in space at the frequency of initiation at their source.

Transition from Phase Waves to Trigger Waves. The preceding discussion has implied that phase waves and trigger waves can be neatly separated from each other. This is not necessarily so in an oscillatory Z reagent. Such a reagent is a continuous medium. Thus diffusive interaction between adjacent points cannot be entirely eliminated. A phase wave is then an idealization that can only be approached as the concentration changes, which result from temporal oscillation at each point in space, become much greater in magnitude than those resulting from diffusion. We have also implied that trigger waves can only occur in a nonoscillatory, but excitable, Z reagent. In fact, an oscillatory Z reagent is also excitable and thus able to support both phase waves and diffusion-dependent trigger waves. We expect that a phase wave traveling in such a Z reagent may initiate a trigger wave. Imagine a very slowly moving phase wave. This would correspond to a situation in which there exists a very steep phase gradient in the direction of propagation such that adjacent points are of greatly different phases. Thus an area undergoing a pulse of ferroin oxidation will be surrounded by areas far away in phase from their own pulses. In such a circumstance these adjacent areas are excitable. The diffusion of Br^- and $HBrO_2$ will cause these areas to experience their pulse of ferroin oxidation prematurely. It is apparent then that a slowly moving phase wave will in fact initiate a trigger wave. We then expect the minimum phase wave velocity in a particular Z reagent to be that of a trigger wave propagating under the same conditions. By a similar mechanism, a pacemaker may initiate a single[15] trigger wave in a synchronously, but slowly, oscillating reagent. Passage of this initial trigger wave will establish a phase gradient. Thus it will be followed by phase waves traveling at the velocity of the initial trigger wave, but appearing at the frequency of temporal oscillation in the medium. It was exactly this phenomenon that Winfree[11e] used to experimentally demonstrate the coexistence of waves with the properties of either phase or trigger waves in a Z reagent. The situation is, however, not completely uncomplicated. The first wave may not be identical with a trigger wave propagating in a nonoscillatory medium. It is not necessarily moving into a region of homogeneous steady state intermediate concentrations; rather, it may propagate into a medium containing residual intermediate concentration gradients resulting from the initially present phase gradient. Furthermore, while the following waves will have all the properties of a phase wave, they will be traveling slowly enough to be affected by diffusion. Winfree[11h] has recognized this fact.

Here we investigate the characteristics of the traveling wave solutions of a set of partial differential equations arising from a model of the reaction-diffusion kinetics of the Z reagent. Analysis is done by means of numerical integration of these partial differential equations. We find traveling wave solutions identifiable as either phase waves or trigger waves mainly on the basis of whether their mechanism of propagation is critically dependent upon diffusion. These waves have the characteristics expected from the preceding discussion. We show that all phase waves of sufficiently slow velocity (steep phase gradient) initiate trigger waves which travel at a velocity mainly characteristic of the particular Z reagent. Numerical values for this velocity are calculated and compared with experimental values.

The Model

The model used here of the chemical kinetics of the Z reagent was initially proposed by Field and Noyes,[16] and it is often referred to as the Oregonator. While the model does not reproduce exactly the quantitative detail of the BZ reaction, it does reproduce qualitative features quite well. Extensive studies of the model indicate that essentially all experimentally observed features of the BZ reaction appear in the Oregonator. This work has been reviewed by Tyson[17] and by Troy.[18]

The model can be written as

$$A + Y \rightarrow X \tag{1}$$

$$X + Y \rightarrow P \tag{2}$$

$$B + X \rightarrow 2X + Z \tag{3}$$

$$X + X \rightarrow Q \tag{4}$$

$$Z \rightarrow fY \tag{5}$$

where $A \equiv B \equiv BrO_3^-$, $X \equiv HBrO_2$, $Y \equiv Br^-$, and $Z \equiv$ ferriin. P and Q are generalized products whose concentrations do not enter into the dynamics of the model because all reactions are assumed to be irreversible. Use of both A and B to represent bromate ion is an attempt to retain generality in the model. Values for the rate constants of reactions 1-4 are assignable[16] by analogy to the FKN mechanism. The rate constant, k_5, and the stoichiometric factor, f, in reaction 5 may be treated as expendable parameters. In this work both of these are usually assigned a numerical value of one. The reaction-diffusion equations describing the dynamics of this model in an unstirred, spatially distributed system are

$$\left(\frac{\partial X}{\partial t}\right)_l = D_X\left(\frac{\partial^2 X}{\partial l^2}\right)_t + k_1AY - k_2XY + k_3BX - 2k_4X^2 \tag{6}$$

$$\left(\frac{\partial Y}{\partial t}\right)_l = D_Y\left(\frac{\partial^2 Y}{\partial l^2}\right)_t - k_1AY - k_2XY + fk_5Z \tag{7}$$

$$\left(\frac{\partial Z}{\partial t}\right)_l = D_Z\left(\frac{\partial^2 Z}{\partial l^2}\right)_t + k_3BX - k_5Z \tag{8}$$

Here X, Y, and Z are the concentrations of the corresponding species, t is time, l is distance, and D_X, D_Y, and D_Z are respectively the diffusion coefficients of X, Y, and Z. It is assumed that $D_X = D_Y = D_Z = D$. It is convenient to recast eq 6-8 into dimensionless variables to give

$$\left(\frac{\partial \alpha}{\partial \tau}\right)_l = D'\left(\frac{\partial^2 \alpha}{\partial l^2}\right)_\tau + s(\eta - \alpha\eta + \alpha + q\alpha^2) \tag{9}$$

$$\left(\frac{\partial \eta}{\partial \tau}\right)_l = D'\left(\frac{\partial^2 \eta}{\partial l^2}\right)_\tau + 1/s(-\eta - \alpha\eta + f\rho) \tag{10}$$

$$\left(\frac{\partial \rho}{\partial \tau}\right)_l = D'\left(\frac{\partial^2 \rho}{\partial l^2}\right)_\tau + w(\alpha - \rho) \tag{11}$$

There is no advantage to introducing a dimensionless distance even though failure to do so leaves D' with the dimension cm^2. Equations defining the new variables are given below.

$$\alpha = \frac{k_2}{k_1A}X \qquad \eta = \frac{k_2}{k_3B}Y \qquad \rho = \frac{k_2k_5}{k_1k_3AB}Z$$

$$\tau = \sqrt{k_1k_3AB}\,t \qquad q = \frac{2k_1k_4A}{k_2k_3B}$$

$$s = \sqrt{k_3B/k_1A} \qquad D' = \frac{D}{\sqrt{k_1k_3AB}}$$

Table I lists the values usually used for the various quantities appearing in these equations. Some rate constants contain $[H^+]$ as a component.

In a spatially distributed, but thoroughly stirred, system

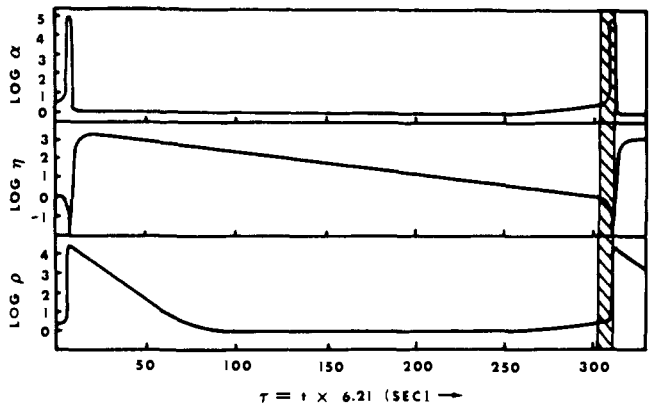

Figure 2. Results of the numerical integration of eq 9-11 with the diffusion terms suppressed. Parameter values used are those in Table I. The kinetic steady state is unstable for these parameter values and oscillation occurs. It is approximately the hatched area that is put onto the grid. The shape of the pulse obscured by the hatching is the same as the earlier pulse. The direction of phase wave propagation translates to from right to left in this diagram.

Table I. Values of Parameters Used in These Calculations[a]

parameter	value	units
k_1	$2.1[H^+]^2$	$M^{-1}\,s^{-1}$
k_2	$2 \times 10^9\,[H^+]$	$M^{-1}\,s^{-1}$
k_3	$1 \times 10^4\,[H^+]$	$M^{-1}\,s^{-1}$
k_4	4×10^7	$M^{-1}\,s^{-1}$
k_5	1	s^{-1}
f	1	none
$[H^+]$	0.8	M
$A \equiv [BrO_3^-]$	0.06	M
$B \equiv [BrO_3^-]$	0.06	M
D	1×10^{-5}	$cm^2\,s^{-1}$

[a] Taken from ref 16.

there are no concentration gradients and the diffusion terms in eq 9-11 approach zero. The system then reduces to the well-understood set of ordinary differential equations[16] modeling the temporal oscillations in the BZ reaction. Figure 2 shows the results of numerical integration of these ordinary differential equations for the parameter values shown in Table I. The steady state is unstable and oscillations appear.

Because for the parameters in Table I the diffusion-independent, chemical reaction portion of eq 9-11 is oscillatory (Figure 2), eq 9-11 may possess traveling wave solutions corresponding to both phase waves and trigger waves. To the extent that the Oregonator model quantitatively reproduces the Z-reagent kinetics, the velocity of the trigger wave solutions should be that observed experimentally. Attempts have been made to calculate the velocity of trigger waves using various simplifications of eq 9-11. The simplifications involve ignoring diffusion of Y and Z and various terms in the chemical kinetic portions of the equations. Tyson[17b] has shown analytically the existence of phase wave solutions in a version of the Oregonator simplified by the assumption $(\partial\alpha/\partial\tau) = 0$. Here we shall solve the complete set of eq 9-11 by numerical integration.

Computational Technique

Method of Lines. The method of lines[19] is a conceptually simple but computationally difficult technique for the numerical solution of sets of partial differential equations. We use the finite difference implementation[20] of the method. In eq 9-11 α, η, and ρ are dependent variables and time (t, $t \propto \tau$) and distance (l) are the independent variables. The method of lines involves a finite discretization of the equations in one of the independent variables, distance in reaction-diffusion

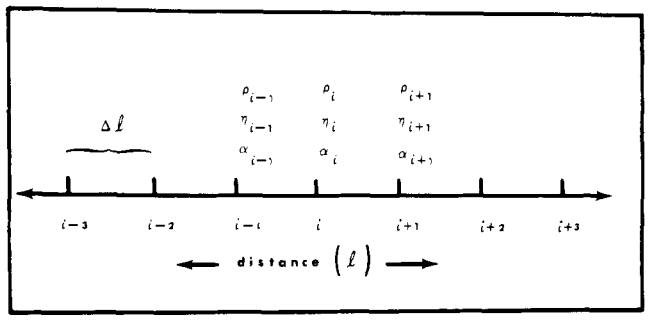

Figure 3. A portion of the grid used in application of the method of lines. The grid point labeling used in eq 12 and 13 corresponds to this figure. Δl is the distance between adjacent grid points. α_i, at a particular grid point.

equations, by generating a grid such as is shown in Figure 3. Then at each point on the grid the derivatives of each dependent variable with respect to the grid variable (l) can be approximated by simple calculation of slopes. Equation 12 shows the expression used to calculate an approximation to the value of $(\partial^2\alpha/\partial l^2)_i$ at space point i.

$$\left(\frac{\partial^2\alpha_i}{\partial l^2}\right)_{t,i} \simeq \frac{\dfrac{\alpha_{i-1}-\alpha_i}{\Delta l} - \dfrac{\alpha_i - \alpha_{i+1}}{\Delta l}}{\Delta l} = \frac{(\alpha_{i-1} - 2\alpha_i + \alpha_{i+1})}{(\Delta l)^2} \tag{12}$$

The term Δl is the distance between grid points. In our implementation, Δl is a constant. However, this is not a necessary requirement of the method. An ordinary differential equation describing the time behavior of each dependent variable at every space point can be formed by making use of this approximation. Equation 13 shows this equation for α_i, i.e., α at space point i.

$$\frac{d\alpha_i}{d\tau} = D'\left(\frac{\alpha_{i-1} - 2\alpha_i + \alpha_{i+1}}{(\Delta l)^2}\right) + s(\eta_i - \alpha_i\eta_i + \alpha_i + q\alpha_i^2) \tag{13}$$

The boundaries of the grid were considered to be impenetrable to diffusion. Normally space grids consisting of 250-1150 points were used in this work. Because there are three dependent variables in this problem, the number of coupled ordinary equations generated by the method of lines is three times the number of grid points. The complete time-space solution to eq 9-11 can then be had by solution of this much larger set of coupled ordinary differential equations.

Methods for the automatic solution of large sets of ordinary differential equations by numerical integration are varied and well developed. Unfortunately, the set of equations resulting from discretization of eq 9-11 is subject to a numerical instability referred to as stiffness.[21] This problem occurs very often in problems in chemical kinetics because of the large range of time constants which may be involved. Furthermore, application of the method of lines to convert a set of partial differential equations to a set of ordinary differential equations often increases stiffness or even introduces stiffness when it was not present before. The practical effect of this difference in time constants is that the time scale of the integration is that of the slower time constants, but the step size must be of the time scale of the faster time constants. Thus most numerical integration algorithms are unable to handle problems involving stiff sets of differential equations because of excessive computer time requirements. However, in the last 10 years much progress has been made in the development of numerical integrations for such problems. Warner[22] has reviewed much of this work. It is the existence of these integrators which now makes the method of lines practicable. We used a variation[23] of an inte-

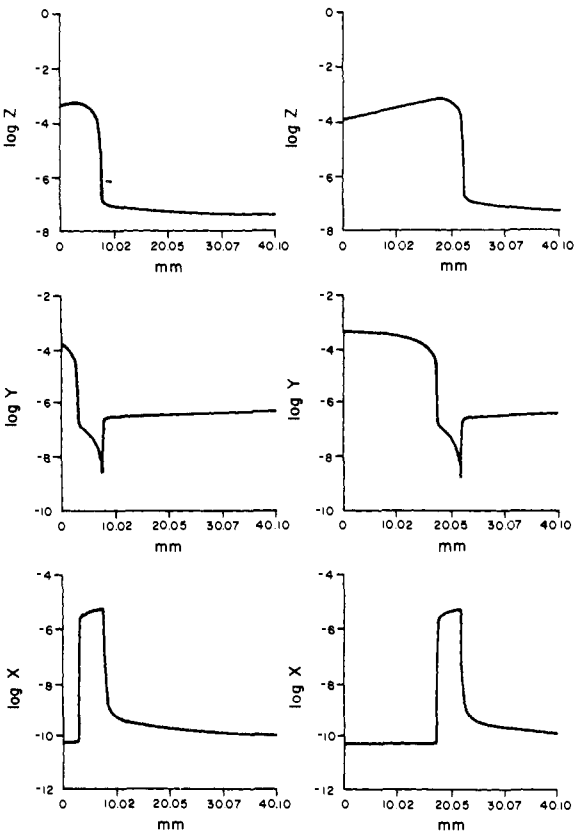

Figure 4. Results of a calculation with $|\nabla\phi| = 0.1$ s/mm. The left-hand side shows the initial wave form at $t = 0.0$ s and the right-hand side shows the wave at $t = 1.4667$ s. The calculated wave velocity is 600 mm/min. This is a phase wave; 250 grid points were used in this calculation. Parameter values were those of Table I.

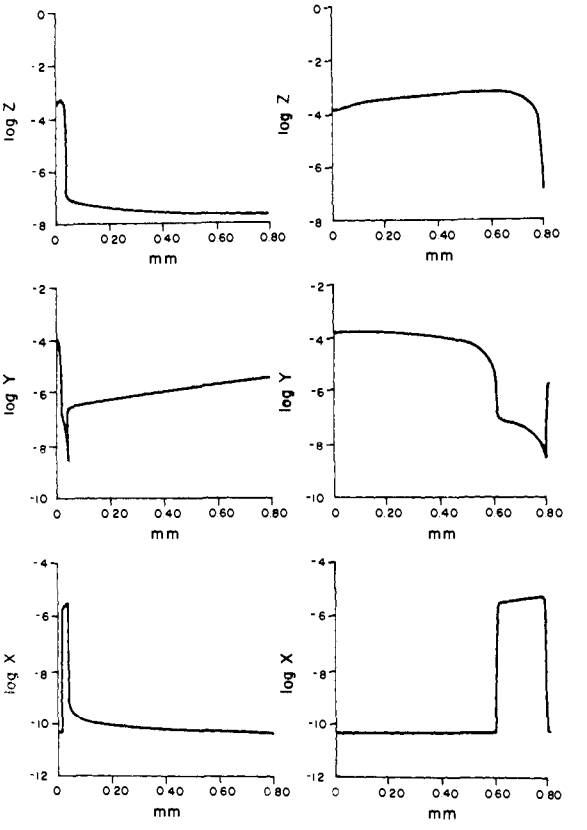

Figure 5. Results of a calculation with initial $|\nabla\phi| = 20$ s/mm. The left-hand side shows the initial wave form at $t = 0.0$ s. The right-hand side shows the diffusion-affected wave form at $t = 1.2410$ s. This is a trigger wave; 1000 grid points were used in the calculation. Parameters were those of Table I.

grator originally devised by Gear.[24] This integrator takes advantage of the banded nature of the Jacobian matrix of sets of equations resulting from application of the method of lines. The integrator automatically monitors numerical stability and keeps global error within defined limits. Calculations were done on the University of Montana DEC-20 computer. Double-precision arithmetic (16 significant figures) was used except that the Jacobian matrix was stored in single precision.

Initial Conditions. Integrations were usually started with a pure phase wave on the grid. The characteristics of this initial phase wave were specified as a phase gradient, $|\nabla\phi|$. The phase gradient, $|\nabla\phi|$, was in turn defined as seconds of the temporal oscillation cycle shown in Figure 2 per millimeter of distance. In transferring this temporal oscillation to the space grid, adjacent points were always separated from their neighbors by 0.1τ or 0.016 10 s of the oscillatory cycle. Thus with 1000 grid points a total of 100τ or 16.10 s in phase is spanned. The total period of the temporal oscillation is 302.8τ or 48.75 s. The section of the oscillation put on the grid was that containing the pulse of ferroin oxidation, i.e., that part corresponding to the wave front. The same wave form was used for all initial $|\nabla\phi|$. Thus for the same number of space points, all initial wave forms appear identical. Differences in $|\nabla\phi|$ are reflected as differences in the assigned magnitude of Δl (Figure 3). In Figure 4 (250 points) $|\nabla\phi|$ is 0.100 s/mm and Δl is 158.73 μm while in Figure 5 (1000 points) $|\nabla\phi|$ is 20 s/mm and Δl is 0.7936 μm. Thus the initial slopes are actually much steeper in Figure 5 than Figure 4.

Results and Discussion

Wave Velocity. The velocity of wave propagation is an important result measured in these calculations. One characteristic of the wave forms obtained which remains unchanged (see Figures 4, 5, 6, 8, and 9) as a wave moves across the grid is the existence of a sharp minimum in Y ($[Br^-]$). This minimum is always clearly assignable to one grid point. Thus it is convenient to use the position of this minimum to calculate the velocity of wave propagation. It is apparent (Figures 4, 5, 6, 8, and 9) that a velocity calculated in this manner is in fact the velocity of wave front movement. It is important to recognize this fact as the wave form itself often changes dramatically as a wave moves across the grid. Movement of the minimum in Y ($[Br^-]$) is discontinuous. It stays at one point for a period of time and then moves abruptly to the next. Division of the distance between grid points by the time between such jumps then yields the wave velocity.

Lower Initial Phase Gradients. Phase Waves. Figure 4 shows the results of a calculation carried out with an initial phase gradient, $|\nabla\phi|$, of 0.1 s/mm. A grid consisting of 250 grid points was used and the parameters were those of Table I. The left-hand side of Figure 4 shows the initial conditions and the right-hand side shows the wave after it has moved 14.667 mm in 1.4667 s.

Recall that for the parameter values of Table I, the mass action kinetics portion of eq 9-11 is oscillatory. For sufficiently low values of $|\nabla\phi|$, adjacent grid points can differ from each other in phase only very slightly. Thus when the wave front (the beginning of the pulse of ferroin oxidation as indicated by the minimum in Y) is at one grid point, it will shortly appear at the next grid point in the direction of wave propagation simply because the small phase gradient ensures that this next grid point will shortly enter the ferroin oxidation portion of its cycle. Because such low $|\nabla\phi|$ waves move rapidly, steep concentration gradients are rather short lived at a particular point in space. These gradients also become less steep as the value of $|\nabla\phi|$ decreases and concentrations at adjacent points become

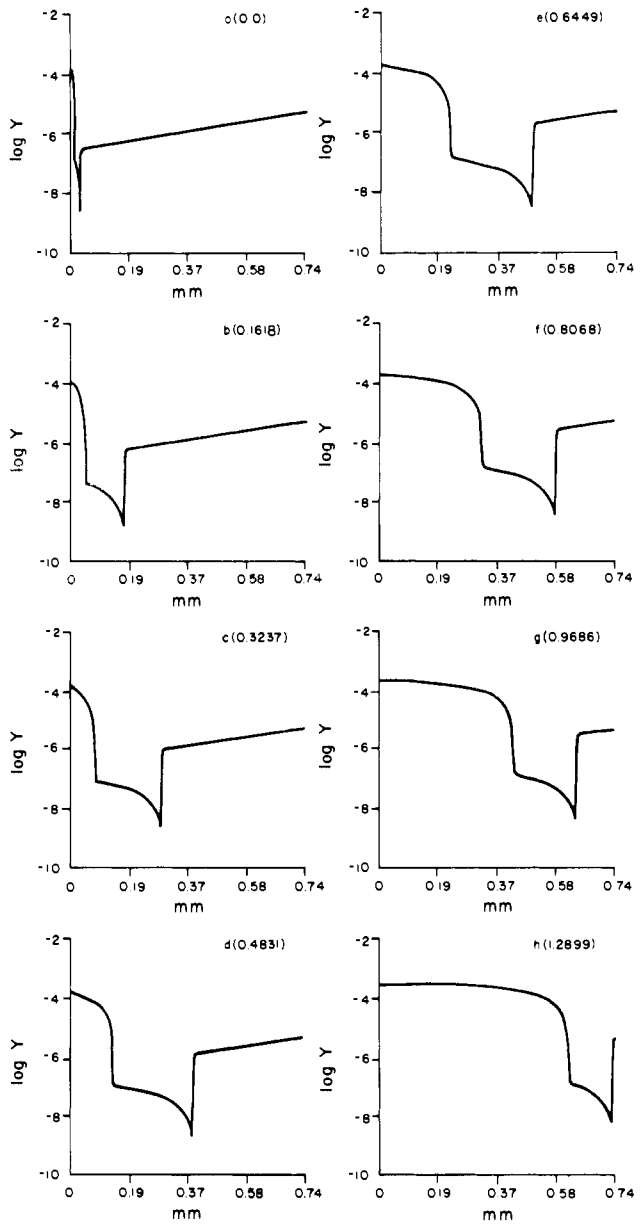

Figure 6. Plots showing the development of the Y ($[Br^-]$) wave form as a trigger wave initiated by a phase wave of $|\nabla\phi| = 25$ s/mm crosses an 1150-point grid. Numbers in parentheses are the times in seconds. The parameters in Table I were used in this calculation.

more similar. For these reasons, at lower values of $|\nabla\phi|$, even around a wave front, concentration changes resulting from temporal oscillation are grossly dominant over those resulting from diffusion. This is apparently the case in the calculation with $|\nabla\phi| = 0.1$ s/mm shown in Figure 4. The initial shape of the wave form is not distorted by diffusion as the wave crosses the grid. Sharp spikes in concentration are not rounded as would be expected if diffusion were important. Furthermore, as closely as we can measure, all dimensions of the wave are unchanging during the calculation.

It is apparent that the velocity of a true phase wave must be constant across the grid and be numerically equal to simply the reciprocal of the phase gradient which it is propagating along. For example, if $|\nabla\phi| = 0.1$ s/mm, an associated phase wave must appear to travel 1 mm in 0.1 s and therefore have a velocity of 10 mm/s or 600 mm/min. This is just the result calculated for the velocity of the wave in Figure 4. Several calculations were done with $0.1 < |\nabla\phi| < 0.8$ mm/s. In all cases waves of constant form moved across the grid with a constant velocity numerically equal to the reciprocal of the initial value of $|\nabla\phi|$. Strong evidence that we are dealing with pure phase waves for $|\nabla\phi| < 0.8$ is supplied by the fact that setting $D' = 0$ in eq 9-11 does not affect the wave velocity or wave form obtained during a calculation. Letting $D' = 0$ is equivalent to placing a barrier impenetrable to diffusion between adjacent pairs of grid points.

We believe that these low $|\nabla\phi|$ waves propagating only by reaction without the influence of diffusion are indeed true phase waves.

Higher Initial Phase Gradients. Trigger Waves. As the initial value of $|\nabla\phi|$ used in these calculations is increased, the results obtained change markedly. Figure 5 shows results obtained for an initial value of $|\nabla\phi|$ of 20 s/mm. The parameters of Table I were used with a grid of 1000 space points. The left-hand side of Figure 5 shows the initial wave form and the right-hand side shows the wave form after the wave front has moved 0.75 mm in 1.2410 s. This high initial $|\nabla\phi|$ wave moves more slowly than the low initial $|\nabla\phi|$ wave shown in Figure 4, but it still moves much more rapidly than the expected phase wave velocity of 3.0 mm/min. The effects of diffusion are apparent in Figure 5. The sharp concentration gradients of the initial wave form have been smoothed, although the Y ($[Br^-]$) minimum has remained localized at one grid point. Even with this smoothing, the wave front is still very sharp. The concentration of Z ([ferriin]) rises from a very low value to its maximum in only about 15 μ. This correlates well with the extreme sharpness[10,11] of the leading edges of the trigger waves observed experimentally in the Z reagent. The changes in wave form in Figure 5 are much more extensive than simply a smoothing. Most importantly, the pulse of ferriin oxidation broadens very considerably between the initial and final forms. These effects of diffusion begin to become apparent at $|\nabla\phi| \sim 1$ s/mm and are dominant at $|\nabla\phi| > 10$ s/mm. Few calculations were done in the intermediate region, $1. < |\nabla\phi| < 10.$

The behavior of diffusion-affected waves such as that of Figure 5 is complex. Neither the wave form nor the wave velocity reaches an unchanging state as the wave crosses the grid. This is demonstrated in Figure 6, which shows the results of a calculation with initial $|\nabla\phi| = 25.0$ s/mm. The parameters of Table I were used with an 1150-point space grid. This is the present capacity of the University of Montana DEC-20 computer. Only the Y ($[Br^-]$) curves are shown in Figure 6 in order to conserve space.[29] The wave front in Figure 6 moved 0.70 mm in 1.2971 s for an overall velocity of 33.93 mm/min. However, the instantaneous velocity varied continuously across the grid.

For $|\nabla\phi| = 25$ s/mm, the expected phase wave velocity is 2.4 mm/min. Figure 7 indicates calculated instantaneous velocities as the wave of Figure 6 propagates across the grid. Figures 6 and 7 are keyed to each other. The vertical lines in Figure 7 indicate the grid position of the Y ($[Br^-]$) minima in the plots of the corresponding letters in Figure 6. The times at which the wave front reached that grid point are noted in parentheses next to the letters in Figure 7. Figure 7 indicates that, initially, the calculated wave velocity increases rapidly from the expected phase wave velocity of 2.4 mm/min to about 50 mm/min. Comparison of Figures 6a and 6b shows that this increase in wave front velocity is accompanied by a large increase in pulse width. Figures 6 and 7 show clearly the initiation of a faster, diffusion-dependent trigger wave by a slower moving phase wave.

Following the initiation of the trigger wave and the accompanying increase in wave velocity, Figure 7 indicates that there is a slow, monotonic decrease in wave front velocity as the wave crosses the grid. After stabilization of the pulse width following trigger wave initiation, this decrease in trigger wave velocity is accompanied by a decrease in pulse width. The plots in Figure 6 suggest that the pulse will eventually be either

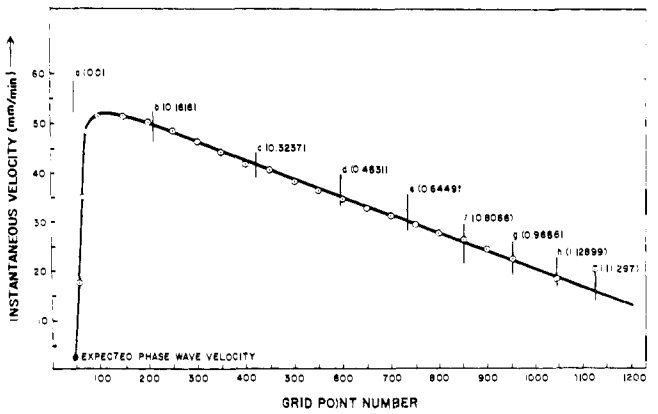

Figure 7. Plot of the instantaneous trigger wave velocity as the wave pictured in Figure 6 crosses the grid. Vertical lines with letters correspond to the times of the Y ([Br^-]) wave forms in Figure 6.

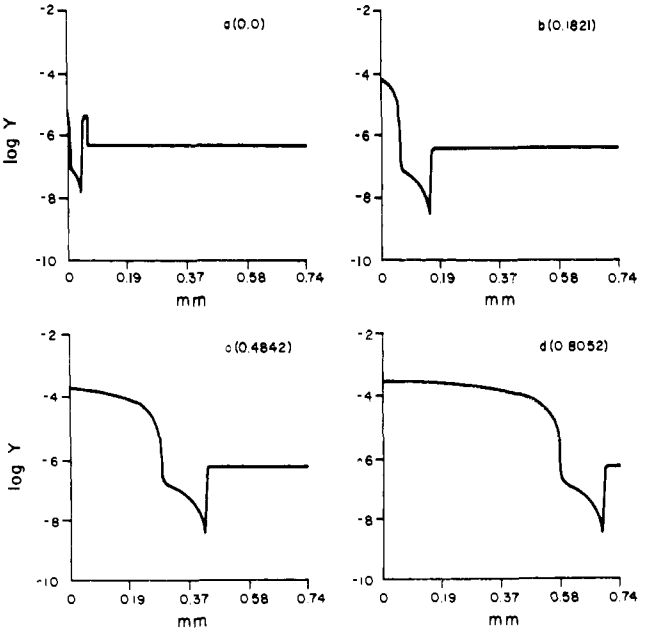

Figure 8. Plots of the Y ([Br^-]) profiles as a trigger wave propagates across in 1150-point grid in a system with a stable steady state. The parameters of Table I were used except that the stable steady state was guaranteed by setting $f = 2.5$. Note the stabilization of the wave form in (c) and (d).

squeezed out of existence or slow to the phase wave velocity, but we have not demonstrated computationally which of these occurs.

We believe that these later changes in wave velocity and pulse width result from the fact that the wave is not moving into an area of spatially homogeneous intermediate concentrations. While X ([$HBrO_2$]) and Z ([ferriin]) do remain relatively constant across the grid, there is a pronounced, monotonic increase in Y ([Br^-]). These varying concentrations are residual effects of the initial phase gradient. They persist because of the low velocity of the corresponding phase wave.

As suggested earlier, trigger waves are most clearly thought of as occurring in a reagent with a stable steady state, in which case the wave propagates into spatially homogeneous intermediate concentrations. In order to demonstrate the properties of such a trigger wave and to support our contention that the decrease in trigger wave velocity and pulse width observed in Figure 7 result from changing intermediate concentrations, calculations were performed using values of f and k_5 such that the steady state is expected to be stable. Setting both time and space derivatives in eq 9-11 equal to zero yields a stability problem identical with the spatially independent system. This problem has been treated in detail.[17,18] For $k_5 = 1.0$, the steady state is stable for values of $f \sim > 1.5$. A value of $f = 2.5$ was used. The initial conditions for these calculations were formed by taking the concentration profiles of the last 92 grid points of a calculation with initial $|\nabla\phi| = 25$ s/mm and $f = 1.0$ after a trigger wave had crossed a 1150-point grid and placing them on the first 92 points of another 1150 space point grid. These points contained the entire pulse of ferroin oxidation including the wave front. The concentrations of X, Y, and Z at the final 1058 grid points were set to their expected steady-state values. The Y ([Br]) profiles resulting from such a calculation are exhibited in Figure 8. Figure 8a shows the initial conditions including a discontinuity resulting from the patchwork nature of the initial wave form. Figures 8c and 8d show that the wave form in this calculation indeed stabilizes. Furthermore, after the initial period of wave form adjustment, the calculated wave velocity reaches a constant value of 49.94 mm/min. As expected, the concentrations of the intermediates remain at their steady-state values until the trigger wave approaches. We conclude that the concentrations of intermediate species, especially Y ([Br^-]), in the area into which a diffusion-dependent trigger wave is propagating affect both the wave form and the wave velocity. This effect is apparent in calculations in which the steady state is unstable and there are concentration gradients residual from an initial phase wave of $|\nabla\phi|$ such that a phase wave would be expected to move much more slowly than the trigger wave which it initiates. In this case there is no unique trigger wave velocity, but the range of velocities observed is not large (see Figure 7) compared to the range of phase wave velocities possible. However, in the case of a system in which there is a stable steady state, intermediate concentrations are constant in all areas not perturbed by the trigger wave, and there are a unique trigger wave velocity and wave form which depend only upon kinetic parameters. The effect of Y ([Br^-]) in the area into which a trigger wave is propagating rationalizes the experimental observation that trigger waves tend to follow each other by a constant increment of space. A following trigger wave will run up the Y ([Br^-]) gradient behind a leading trigger wave until the following wave slows to the velocity of the leading wave. The decrease in pulse width with increasing Y ([Br^-]) at the wave front suggests that there exists a value of Y ([Br^-]) high enough for an area to be impenetrable to a trigger wave, as is observed experimentally.

One final calculation was carried out to emphasize the uniqueness of a trigger wave in a system with a stable steady state. In this calculation 1150 space points were used with the parameters of Table I except that $f = 2.5$. The values of X ([$HBrO_2$]) and Z ([ferriin]) were set initially equal to their steady-state values at all grid points. The value of Y ([Br^-]) was set to its steady-state value ($Y = 5.25 \times 10^{-7}$ M) at all grid points except for 28-48, which were set at 4.63×10^{-9} M, and 49, which was set at 3.133×10^{-9}. This latter point was set to be the minimum in order to avoid confusing the velocity calculation algorithm. Except for the initial conditions, the calculations of Figures 8 and 9 are identical. The left-hand side of Figure 9 shows this initial condition. The right-hand side of Figure 9 shows that a perturbation of this magnitude is sufficient to initiate a trigger wave. The form of this trigger wave is exactly identical with that of the trigger wave shown in Figure 8 which had a close approximation to a trigger wave as its initial condition. Furthermore, the velocity of the trigger wave in Figure 9 is exactly that of the trigger wave in Figure 8, 49.94 mm/min. We did not investigate systematically the magnitude of the initial perturbation necessary to initiate a trigger wave in a system at its steady state. We did find, however, that similar perturbations in Y ([Br^-]) affecting only five space points decayed quickly back to the steady state.

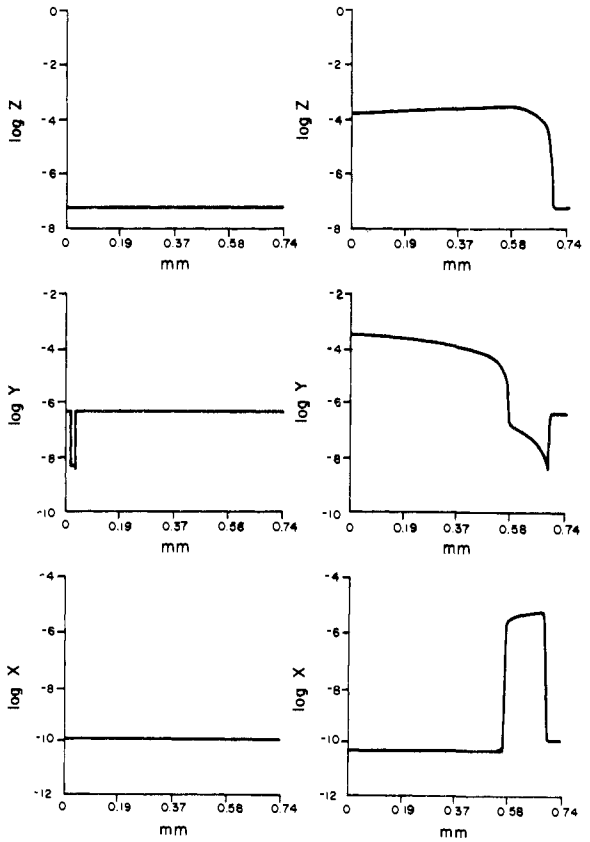

Figure 9. Plots of the three intermediate concentrations for a calculation identical with that of Figure 8 except that the initial conditions used were the steady-state perturbation shown on the left-hand side here rather than the already formed wave used in the calculation of Figure 8. Note that the final Y ([Br$^-$]) wave form obtained here is identical with that shown in Figure 8.

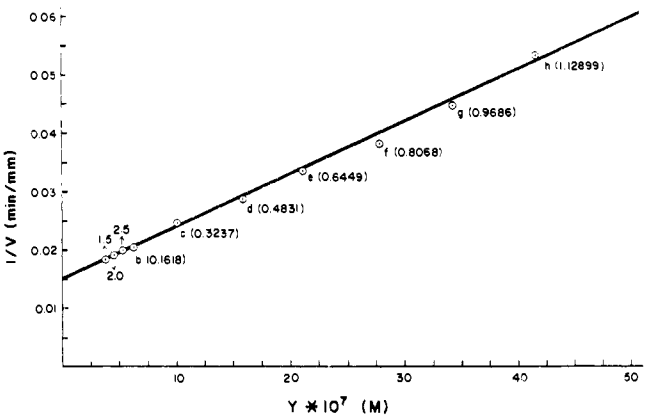

Figure 10. Plot of the reciprocal of instantaneous trigger wave velocity vs. the value of $Y \equiv$ [Br$^-$] just at the wave front. Points identified with numbers refer to steady-state calculations with f equal to the identifying number.

The consistency and reasonableness of the results obtained strengthen our confidence that the methods used here do indeed yield accurate solutions to eq 9-11. No calculation led to results not easily rationalizable on the basis of the chemistry involved. All tests of reproducibility were successful. Furthermore, our results are invariant to grid size above 50 points. There is a boundary effect which seems to penetrate about 20 points into the grid. The slight dip in Z ([ferriin]) noticeable on the right-hand side of Figure 5 is an example of this boundary effect. We do not know whether or not this is an artifact of the calculation; there are certainly boundary effects observed experimentally in the Z reagent. The results of our calculations are also independent of the error tolerance used. Tightening the error parameter to 10^{-8} had no effect other than increasing the computation time. Loosening this parameter to 10^{-4} only introduces damped oscillations in X ([$HBrO_2$]) at the end of the pulse of oxidation. Normally an error tolerance of 10^{-5} was used in these calculations.

Velocity of Trigger Wave Propagation. The calculations carried out here were done with parameters (Table I) based upon the reactant concentration values [BrO_3^-] = 0.06 M and [H^+] = 0.8 M. The concentrations of only these reactants appear in the Oregonator model. Field and Noyes[10] have determined experimentally that only these concentrations affect at all strongly the observed velocity of trigger wave propagation. They also observed a trigger wave velocity of 5.4 mm/min for the reactant concentrations of Table I. It is of interest to compare our calculated trigger wave velocities with the experimentally observed and to previously calculated values.

Comparison of our calculated trigger wave velocities with the experimental is not straightforward because the calculated values depend upon the magnitude of Y ([Br$^-$]) in the area into which the wave is propagating. Figure 10 shows this dependence. Figure 10 is partially keyed to Figure 6; points with letters relate to the velocities at the corresponding plots in Figure 6. The three points in Figure 10 labeled with numbers are from steady-state calculations. The numbers give the value of f used. The calculated dependence of trigger wave velocity (V) upon the value of Y ([Br$^-$]) at the wave front is given by

$$1/V = k' + kY \qquad (14)$$

The values of k and k' determined from Figure 10 are respectively 9180 min/mm·M and 0.015 min/mm. We attach no particular significance to this relationship except the obvious one that the velocity is roughly inversely dependent upon Y ([Br$^-$]). The range of calculated velocities if from about 18 to 54 mm/min. We have experimentally determined that the actual steady-state concentration in a nonoscillatory Z reagent of the composition corresponding to our calculations is about 4×10^{-6} M. This is considerably above the steady-state concentrations calculated on the basis of eq 9-11. The calculated velocity in Figure 10 which corresponds to the experimental steady-state Y ([Br$^-$]) is about 25 mm/min. This value is about five times larger than observed. However, this result is considered to be in excellent agreement with the experimental value because earlier work[3] suggests that the estimated value of k_3/k_1 used here is about three times too high. It is this rate constant ratio which is expected to have the greatest effect upon trigger wave velocity and the discrepancy observed here is in the correct direction to arise from the error in k_3/k_1. It is apparent in these calculations that the trigger wave velocity is quite sensitive to kinetic parameters. The discrepancies noted here probably result from two approximations implicit in the Oregonator. The first involves reaction 5 (eq 5). This simple step attempts to model the very complex and still not completely understood[4] interaction of ferriin with malonic and bromomalonic acids. The values of f and k_5 used here are essentially arbitrary because it is very difficult to relate them directly to the actual chemistry involved. It is very likely this step which leads to the low steady-state bromide ion concentrations calculated from the Oregonator. The model of Edelson, Noyes, and Field[5] adds considerable detail to step 5, but this model is too complex for our present computational facilities. The second approximation implicit in the Oregonator involves the assumption of irreversibility of all steps. Barkin, Bixon, Bar-Eli, and Noyes[25] have demonstrated that reversibility is important at least in reaction 3 (eq 3) of the Oregonator. This reversibility is expected to lead to a lower calculated trigger wave velocity. A reversible version of the Oregonator has been proposed by Field[26] and we are now extending our

calculations to this model. One final point to be made is that it is known[11e] that air has the effect of stabilizing the steady state of a sample of Z reagent spread in a thin layer in contact with the atmosphere. This effect must be accompanied by an increase in bromide ion concentration, but this is not taken into account by the Oregonator.

Several previous attempts have been made to calculate a trigger wave velocity from truncated versions of eq 9-11. We have normalized these results to the parameter values of Table I. Field and Noyes[10] calculated a velocity assuming that only diffusion of $HBrO_2$ and its autocatalytic formation in reaction 3 are important to trigger wave propagation. Thus they solved the equation

$$\left(\frac{\partial X}{\partial t}\right)_l = D_x \left(\frac{\partial^2 X}{\partial l^2}\right)_t + k_3 AX \qquad (15)$$

analytically for the sharpest wave front and calculated a wave velocity about 15 times higher than observed. Tilden[27] further reasoned that destruction of X by Y in the wave front must affect trigger wave velocity and took this into account using the equation

$$\left(\frac{\partial X}{\partial t}\right)_l = D_x \left(\frac{\partial^2 X}{\partial l^2}\right)_t + k_3 AX - k_2 XY_0 \qquad (16)$$

He found that by adjusting Y_0, the value of Y exactly at the wave front, within a physically reasonable range of $Y = 10^{-7}$-10^{-6} M, the experimentally observed trigger wave velocity could be exactly reproduced. Our calculations support Tilden's view of the importance of bromide ion concentration in the wave front. Field and Troy[28] calculated a trigger wave velocity using a version of eq 9-11 obtained by setting $D_y = D_z = 0$. This takes into account the presence of Y in the wave front but not its diffusion. Because of the need for a globally stable steady state, Field and Troy's methods are only applicable to systems with $f > 2.414$. For a calculation using the same parameters as those used here to generate Figure 8, they obtained an essentially identical trigger wave velocity. They further showed both numerically and analytically that the trigger wave velocity obtained is unique for a particular set of parameters, just as we have found here.

Conclusion

We have used numerical techniques to investigate the partial differential equations representing the reaction-diffusion dynamics of the Oregonator model of the Z reagent. We find traveling wave solutions. These correspond to either phase waves or trigger waves. Phase waves appear when the chemical kinetic portion of the reaction-diffusion equations is oscillatory. They travel at a velocity simply equal to the reciprocal of the initial phase gradient. They are unaffected by diffusion. Trigger waves may appear when the kinetic portion of the reaction-diffusion equations is either oscillatory or merely excitable. These waves are diffusion dependent. If the kinetic portion of the reaction-diffusion equations is stable and nonoscillatory, then intermediate concentrations are homogeneous in space. In this case, a trigger wave travels at a constant velocity uniquely determined by the kinetic and diffusive parameters of the system. If the kinetic portion of the reaction-diffusion equations is oscillatory, then both phase waves and trigger waves may appear. However, a phase wave traveling more slowly than a trigger wave would under the same conditions initiate this trigger wave. Under this circumstance the trigger wave velocity is not constant but is instead affected by spatial changes in bromide ion concentration residual from the phase gradient that the original phase wave was propagating along. An increase in bromide ion concentration at the wave front leads to a decrease in trigger wave velocity. It is also shown here that a sufficiently large perturbation of a system in a steady state may lead to the formation of a trigger wave which then travels at the unique velocity defined by the kinetic and diffusive parameters of the system. Agreement between calculated and observed trigger wave velocities is satisfactory. Suggestions are made for the improvement of the kinetic model.

Acknowledgments. This paper benefited from critical readings by David Vanecek and especially by Arthur T. Winfree. R. J. F. wishes to thank the University of Montana Small Grants Program for summer support in 1976 and 1977. This work would not have been possible without the help and cooperation of the University of Montana Computer Center. Its Director, Steve Henry, made room for us on the system and consultants Dan Ballas, Marge Baker, and Jim Ullrich supplied invaluable technical assistance. Parts of this work were supported by the NSF under Grant CHE77-03599.

References and Notes

(1) Floating Point Systems, Beaverton, Oregon.
(2) B. P. Belousov, *Ref. Radiats, Med. 1958, Medgiz, Moscow*, 145 (1959); A. M. Zhabotinskii, *Dokl. Akad. Nauk. SSSR.* **157**, 392 (1964).
(3) R. J. Field, E. Körös, and R. M. Noyes, *J. Am. Chem. Soc.*, **94**, 8649 (1972).
(4) R. J. Field, "Theoretical Chemistry: Advances and Perspectives", Vol. 4, Academic Press, New York, 1978, p 54.
(5) D. Edelson, R. M. Noyes, and R. J. Field, *Int. J. Chem. Kinet.*, in press.
(6) A. N. Zaikin and A. M. Zhabotinskii, *Nature (London)*, **225**, 535 (1970).
(7) Ferroin is the tris(1,10-phenanthroline)iron(II) ion. It is red. Ferriin is the tris(1,10-phenanthroline)iron(III) ion. It is blue. All BZ catalysts are metal ions or complexes able to undergo one-electron redox processes.
(8) H. Wolfe and R. J. Field, Department of Chemistry, University of Montana, unpublished results, 1977.
(9) R. P. Rastogi, K. Yadava, and K. Prasad, *Indian J. Chem.*, **13**, 352 (1975).
(10) R. J. Field and R. M. Noyes, *J. Am. Chem. Soc.*, **96**, 2001 (1974).
(11) (a) A. T. Winfree, *Science*, **175**, 634 (1972); (b) *ibid.*, **181**, 937 (1973); (c) *Math, Probl. Biol., Lect. Notes Biomath.*, **2**, 241 (1974); (d) H. Mel, Ed., "Science and Humanism: Partners in Human Progress", University of California Press, Berkeley, 1974; (e) *Faraday Symp., Chem., Soc.*, **9**, 38 (1974); (f) *SIAM-AMS Proc.* **8**, *77113 (1974)*; (g) *Sci. Am.*, **230**, 82 (1974); (h) book in preparation.
(12) J. Dayantis and J. Sturm, *C. R. Acad. Sci., Ser. C*, **280**, 1447 (1975).
(13) N. Kopell and L. N. Howard, *Science*, **180**, 1171 (1973).
(14) D. Thoenes, *Nature (London), Phys. Sci.*, **243**, 18 (1973).
(15) K. Showalter and R. M. Noyes, *J. Am. Chem. Soc.*, **98**, 3730 (1976).
(16) R. J. Field and R. M. Noyes, *J. Chem. Phys.*, **60**, 1877 (1974).
(17) (a) J. J. Tyson, *Lect. Notes Biomath*, **10** (1976); (b) *J. Chem. Phys.*, **66**, 905 (1977).
(18) W. C. Troy in ref 4, p 133.
(19) A. O. Liskovets, *Differential Equations*, **1**, 1308 (1965).
(20) D. Edelson and N. L. Schryer, *Comput. Chem.*, in press.
(21) J. O. Hirschfelder, *J. Chem. Phys.*, **26**, 271 (1952).
(22) D. Warner, *J. Phys. Chem.*, **81**, 2329 (1977).
(23) A. C. Hindmarsh, Lawrence Livermore Laboratory, Report UCID-30059, Rev. 1, "Solution of Ordinary Differential Equations Having Banded Jacobian". Program available as ACC No. 661 from Argonne Code Center, Argonne, Ill 60439.
(24) C. W. Gear, "Numerical Initial Value Problems in Ordinary Differential Equations", Prentice-Hall, Englewood Cliffs, N.J., 1971, p 209 ff.
(25) S. Barkin, M. Bixon, K. Bar Eli, and R. M. Noyes, *Int. J. Chem. Kinet.*, **9**, 841 (1977).
(26) R. J. Field, *J. Chem. Phys.*, **63**, 2289 (1975).
(27) J. Tilden, *J. Chem. Phys.*, **60**, 3349 (1974).
(28) R. J. Field and W. C. Troy, *SIAM J. Appl. Math.*, in press.
(29) A complete set of plots for any calculation discussed in this paper may be obtained from the authors.